Article

Multidrug-Binding Transcription Factor QacR Binds the Bivalent Aromatic Diamidines DB75 and DB359 in Multiple Positions

Benjamin E. Brooks, Kevin M. Piro, and Richard G. Brennan

J. Am. Chem. Soc., **2007**, 129 (26), 8389-8395• DOI: 10.1021/ja072576v • Publication Date (Web): 13 June 2007

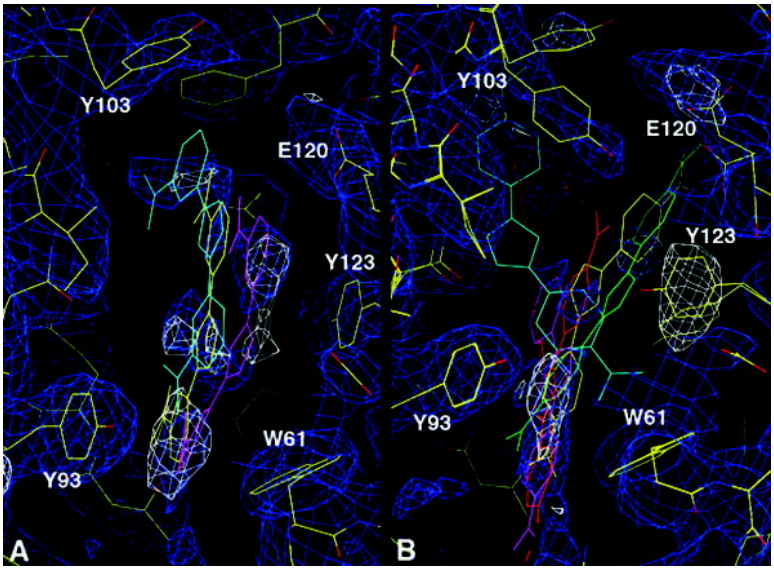

More About This Article

Additional resources and features associated with this article are available within the HTML version:

- Supporting Information
- Links to the 2 articles that cite this article, as of the time of this article download
- Access to high resolution figures
- Links to articles and content related to this article
- Copyright permission to reproduce figures and/or text from this article

View the Full Text HTML

J|A|C|S
ARTICLES
Published on Web 06/13/2007

Multidrug-Binding Transcription Factor QacR Binds the Bivalent Aromatic Diamidines DB75 and DB359 in Multiple Positions

Benjamin E. Brooks, Kevin M. Piro, and Richard G. Brennan*

Contribution from the Department of Biochemistry and Molecular Biology, University of Texas MD Anderson Cancer Center, Unit 1000, 1515 Holcombe Boulevard, Houston, Texas 77030

Received April 12, 2007; E-mail: rgbrenna@mdanderson.org

Abstract: *Staphylococcus aureus* QacR is a multidrug-binding transcription repressor. Crystal structures of multiple QacR−drug complexes reveal that these toxins bind in a large pocket, which is composed of smaller overlapping "minipockets". Stacking, van der Waals, and ionic interactions are common features of binding, whereas hydrogen bonds are limited. Pentamidine, a bivalent aromatic diamidine, interacts with QacR differently as one positively charged benzamidine moiety is neutralized by the dipoles of side-chain and peptide backbone oxygens rather than a formal negative charge from proximal acidic residues. To understand the binding mechanisms of other bivalent benzamidines, we determined the crystal structures of the QacR−DB75 and QacR−DB359 complexes and measured their binding affinities. Although these rigid aromatic diamidines bind with low-micromolar affinities, they do not use single, discrete binding modes. Such promiscuous binding underscores the intrinsic chemical redundancy of the QacR multidrug-binding pocket. Chemical redundancy is likely a hallmark of all multidrug-binding pockets, yet it is utilized by only a subset of drugs, which, for QacR, so far appears to be limited to chemically rigid, bivalent compounds.

Introduction

QacR is a multidrug-binding transcription regulator that represses the expression of the plasmid-encoded multidrug efflux transporter gene *qacA*.[1] The QacA pump confers resistance to multiple monovalent and bivalent aromatic antibiotics, antiseptics, and disinfectants, many of which are quaternary ammonium compounds (QACs), in the human pathogen *Staphylococcus aureus*.[2] QacR binds and is induced by many of the same lipophilic monovalent and bivalent cationic cytotoxins and thereby acts as a cytosolic drug sensor. QacR belongs to the TetR family[3] and is an all-helical homodimer. The first three helices comprise the DNA-binding domain and the last six helices, the dimerization interface and multidrug-binding pocket.[1,4,5] Upon drug binding a coil-to-helix transition of residues 89−93 results in the expulsion of residues Y92 and Y93 from the interior of the protein and formation of a large multidrug-binding pocket with a volume of ∼1100 Å^3.[5] This conformational change is transduced to the distal DNA-binding domain and results in the rotation and translation of the helix-turn-helix motif and subsequent inability of QacR to bind cognate DNA. Interestingly, the stoichiometry of drug binding is one drug per QacR dimer, in which the drug-bound subunit undergoes a dramatic conformational change including an ∼37° rotation and ∼10 Å translation of the DNA-binding domain. The drug-free subunit undergoes a much smaller concomitant rotation and translation.[4,5] Although the apo form has not been shown to be amenable to crystallization alone, it is fortuitous that a second QacR dimer is found in the asymmetric unit of the drug-bound crystal form of QacR. The multidrug-binding pocket of this drug-free QacR dimer is nearly identical to that of the DNA-bound conformation of QacR, the hallmarks of which are the complete burial of residues Y92 and Y93 inside the hydrophobic core of the protein and no coil-to-helix transition.[4,5]

The multidrug-binding pocket of drug-bound QacR is composed of a series of overlapping "minipockets" that host multiple, differently shaped cationic, lipophilic cytotoxins. Ethidium (Et) and rhodamine 6G (R6G) binding define two of the smaller pockets, the so-named "R6G" and "Et" pockets, which are located at opposite ends of the larger ligand-binding pocket.[5] Dequalinium, a bivalent compound, and malachite green, a propeller-shaped monovalent aromatic, span both pockets but do so in distinct fashion.[5] In order to bind all of these chemically and structurally different ligands, multiple residues are utilized that maximize protein−drug interaction. Two critical residues are Y103 and Y123, which rotate about their χ1 and χ2 torsion angles in order to accommodate different drugs. Another feature of the multidrug-binding pocket of QacR, and in accord with its selectivity for aromatic monovalent and bivalent *cationic* drugs, is its highly acidic nature due to the presence of glutamate residues E57, E58, E63, E90, and E120.

(1) Grkovic, S.; Brown, M. H.; Roberts, N. J.; Paulsen, I. T.; Skurray, R. A. *J. Biol. Chem.* **1998**, *273*, 18665−18673.
(2) Paulsen, I. T.; Brown, M. H.; Littlejohn, T. G.; Mitchell, B. A.; Skurray, R. A. *Proc. Natl. Acad. Sci. U.S.A.* **1996**, *93*, 3630−3635.
(3) Ramos, J. L.; Martinez-Bueno, M.; Molina-Henares, A. J.; Teran, W.; Watanabe, K.; Zhang, X.; Gallegos, M. T.; Brennan, R.; Tobes, R. *Microbiol. Mol. Biol. Rev.* **2005**, *69* (2), 326−356.
(4) Schumacher, M. A.; Miller, M. C.; Grkovic, S.; Brown, M. H.; Skurray, R. A.; Brennan, R. G. *EMBO J.* **2002**, *21*, 1210−1218.
(5) Schumacher, M. A.; Miller, M. C.; Grkovic, S.; Brown, M. H.; Skurray, R. A.; Brennan, R. G. *Science* **2001**, *294*, 2158−2163.

10.1021/ja072576v CCC: $37.00

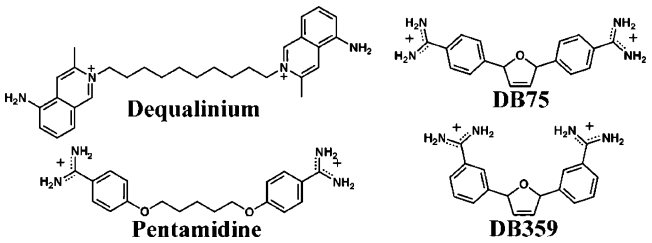

Figure 1. Chemical structures of bivalent lipophilic compounds that bind to QacR.

The carboxylates of these residues interact selectively with the positive charges of each drug. For example, E90 interacts with R6G and E120 with Et, whereas berberine and proflavin, both of which bind in the R6G pocket, interact with E57 and E58.[5,6]

For the greater part, drugs bind to QacR in the R6G or Et pockets. However, the bivalent drug, pentamidine (Figure 1), takes a different binding mode in which one end of the drug protrudes from the binding pocket to the surface of the protein where it interacts with residue E63.[7] The other benzamidine group remains buried but is "neutralized" primarily by its interactions with the hydroxyl group of Y127 and negative dipoles of the carbonyl oxygen atoms of the peptide backbone rather than a carboxylate. Overall the drug is rather twisted. By contrast, hexamidine, which is simply one methylene group longer than pentamidine, binds to QacR in an extended manner similar to that of dequalinium.[7] Moreover, the two positive charges on hexamidine are neutralized by the side chains of acid residues E57 and E120.

Given the different binding modes of pentamidine and hexamidine, we chose to characterize the interactions of QacR with two additional bivalent aromatic benzamidines, DB75 and DB359 (Figure 1). Both compounds are slightly smaller and significantly more rigid than pentamidine and hexamidine. Similar to pentamidine, DB75 is a potent DNA-binding drug that exhibits topoisomerase II inhibition and antigiardial activities.[8,9] However, the different shape of DB359 does not allow for potent DNA binding.[8,10] Isothermal titration calorimetry was utilized to determine the binding affinities of these compounds for QacR and X-ray crystallography to provide atomic details of their binding. The data reveal that indeed DB75 and DB359 are QacR ligands, albeit those with modest affinities, which surprisingly bind in the large QacR binding pocket in multiple, apparently isoenergetic orientations.

Materials and Methods

Mutagenesis and Expression Constructs. Wild-type and genetically modified *qacR* genes were cloned into the recombinant expression vector pTTQ18 and used to produce protein for these experiments as described previously.[1,11] For better protein production in *E. coli*, all QacR expression constructs were codon optimized and two nonessential cysteines were modified (C72A/C141S). No effect on drug or DNA-binding activity is observed.[11] A C-terminal hexahistadine tag was added to allow purification of the protein by nickel−nitrolotriacetic acid−agarose (Ni−NTA) affinity column chromatography (Qiagen, Valencia, CA).[1]

Protein Expression and Purification. The protein expression and purification protocols were modified slightly from previous publications.[1,11] Protein expression was induced in *E. coli* DH5α cells with 0.5 mM IPTG in the mid log growth phase (~0.6 OD_{590}). After 3−5 h of additional incubation, cells were harvested and stored at −20 °C. Thawed cell paste was resuspended in 30 mL of buffer A (50 mM Tris-HCl, 50 mM imidazole, 300 mM NaCl, and 5% glycerol, pH 7.5). After the addition of 500 μg of DNAse I, the cells were lysed by French press at 4 °C. Cell debris was removed by centrifugation, and the supernatant was loaded onto a Ni−NTA affinity column, which was pre-equilibrated with buffer A. The column was washed first with 100 mL of buffer A and then with 100 mL of buffer A with 100 mM imidazole. The protein was eluted with buffer A with 1.0 M imidazole. Purity was assessed by SDS−polyacrylamide gel electrophoresis and coomassie blue staining. The best fractions, those of greater than 95% purity, were pooled and concentrated.

Crystallization. For reproducible crystallization of the drug-bound conformation of QacR, reductive alkylation of the lysines of the purified protein is necessary. The protocol that was published previously was followed.[5,12] The extra imidazole from protein purification and the byproducts from reductive alkylation were removed by three buffer exchanges with dilutions of at least 1:10 into buffer A. Before setting up hanging drop−vapor diffusion crystallization experiments with ligands DB75 and DB359, solutions of purified QacR were incubated with 200−500 μM ligand or more commonly incubated with a saturating amount of each ligand overnight at 4 °C. Any resulting precipitate was removed by centrifugation. The clarified supernatants, which contained each drug−QacR complex, were used in all subsequent crystallization experiments. Ten microliter hanging drops, which included equal volumes of protein with ligand in buffer A and reservoir buffer (2.3 M ammonium sulfate and 0.1 M sodium acetate, pH 4.6 to 5.0), were sealed over 1 mL of reservoir buffer. Crystals took between 4 days and 2 weeks to reach full size and grew as rectangular prisms. Crystals of each complex took the space group $P4_22_12$ and were isomorphous to all other QacR−drug complex crystals reported to date.[5−7]

X-ray Intensity Data Collection. X-ray diffraction data were collected at 100 K at beamline 8.2.1 of the Advanced Light Source (ALS) in Berkeley, CA. The cryoprotectant contained 1.6 M ammonium sulfate, 0.1 M sodium acetate, and 20% glycerol. These data sets were collected using the Blu-Ice control program, and intensity data integration and scaling were done with MOSFLM and SCALA as implemented in the software package CCP4.[13] Selected crystallographic statistics are listed in Table 1.

Structure Determination and Refinement. The structures of the DB75−QacR and DB359−QacR complexes were solved using the molecular replacement program MOLREP as implemented in CCP4 and the QacR−dequalinium complex structure (with drug and solvent removed) as the search model.[5,13] The ligand coordinates as well as the related stereochemistry files for use with the program O and topology and parameter files used with CNS (Crystallography and NMR System) were obtained from the Hetero-compound Information Centre-Uppsala (Hic-Up server; http://alpha2.bmc.uu.se/hicup/).[14−16] The

(6) Schumacher, M. A.; Miller, M. C.; Brennan, R. G. *EMBO J.* **2004**, *23*, 2923−2930.
(7) Murray, D. S.; Schumacher, M. A.; Brennan, R. G. *J. Biol. Chem.* **2004**, *279*, 14365−14371.
(8) Nguyen, B.; Lee, M. P. H.; Hamelberg, D.; Joubert, A.; Bailly, C.; Brun, R.; Neidle, S.; Wilson, D. W. *J. Am. Chem. Soc.* **2002**, *124*, 13680−13681.
(9) Boykin, D. W.; Kumar, A.; Xiao, G.; Wilson, W. D.; Bender, B. C.; McCurdy, D. R.; Hall, J. E.; Tidwell, R. R. *J. Med. Chem.* **1998**, *41*, 124−129.
(10) Chaires, J. B.; Ren, J.; Hamelberg, D.; Kumar, A.; Pandya, V.; Boykin, D. W.; Wilson, W. D. *J. Med. Chem.* **2004**, *47*, 5729−5742.
(11) Grkovic, S.; Brown, M. H.; Schumacher, M. A.; Brennan, R. G.; Skurray, R. A. *J. Bacteriol.* **2001**, *183*, 7102−7109.
(12) Rayment, I. *Methods Enzymol.* **1997**, *276*, 171−179.
(13) The CCP4 Suite: Programs for Protein Crystallography. *Acta Crystallogr., Sect. D: Biol. Crystallogr.* **1994**, *50*, 760−763.
(14) Kleywegt, G. J.; Jones, T. A. *Acta Crystallogr., Sect. D* **1998**, *54*, 1119−1131.
(15) Brünger, A. T.; Adams, P. D.; Clore, G. M.; DeLano, W. L.; Gros, P.; Grosse-Kunstleve, R. W.; Jiang, J. S.; Kuszewski, J.; Nilges, M.; Pannu, N. S.; Read, R. J.; Rice, L. M.; Simonson, T.; Warren, G. L. *Acta Crystallogr., Sect. D: Biol. Crystallogr.* **1998**, *54*, 905−921.
(16) Jones, T. A.; Zou, J. Y.; Cowan, S. W.; Kjeldgaard, M. *Acta Crystallogr., Sect. A* **1991**, *47*, 110−119.

Table 1. Selected Crystallographic Data

	QacR–DB75	QacR–DB359
space group	$P4_22_12$	$P4_22_12$
cell constants (Å)	172.0	171.4
	172.0	171.4
	94.6	94.5
resolution range (Å)	76.7−2.80	63.5−2.80
highest resolution shell (Å)	2.98−2.80	3.00−2.80
R_{work} (%)[a]	22.4	21.3
R_{free} (%)[b]	28.9	25.9
$I/\sigma(I)$	5.2 (2.0)[c]	10 (1.9)
completeness (%)	98.5 (96.0)	96.2 (88.7)
R_{sym} (%)[d]	7.7 (37.7)	5.2 (41.2)
total reflections (no.#)	116154	170971
unique reflections (no.)	34470	33907
multiplicity	3.4	5.1
rmsd		
bond angles (deg)	1.2	1.2
bond lengths (Å)	0.008	0.008
main chain B values (Å^2)	1.6	1.3
solvent		
water (no.)	6	24
sulfate (no.)	8	12
Ramachandran analysis		
most favored (%)	84.7	89.1
additional allowed (%)	13.9	9.7
generously allowed (%)	0.6	0.4
disallowed (%)	0.9	0.7
CV−Luzzati coordinate error	0.48	0.44

[a] $R_{work} = (\sum|F_{obs} - F_{calc}|)/|F_{obs}|$, where $F_{obs} - F_{calc}$ are the observed and calculated structure factors, respectively. [b] $R_{free} = R_{work}$ for 5% of all structure factors that were selected randomly for cross-validation purposes. [c] Values in parentheses are the statistics for the highest resolution shell of data. [d] $R_{sym} = \sum|I_{hkl} - \langle I\rangle|/\sum\langle I\rangle$, where $\langle I\rangle$ is the average individual measurement of I_{hkl}.

program O was used to visualize and manipulate the experimental electron density maps and structures for model building. CNS was used for all refinements of the crystal structures and model assessment.

Refinement consisted of an initial round of rigid body refinement followed by two rounds of simulated annealing. Positional refinement followed, and all subsequent adjustments to the structures, including the addition of sulfate and water molecules, were made by fitting and rebuilding into a series of $2F_o - F_c$ and $F_o - F_c$ electron density maps. In addition to van der Waals and hydrogen-bonding distance constraints, the following overlapping electron density criteria were used for solvent, ion, and ligand placement: $2F_o - F_c > 1.0\sigma$ and $F_o - F_c > 3.0\sigma$. After each refinement converged, $(2F_o - F_c)$ simulated annealing composite omit maps were used to verify the final model. Models were validated with the "model check" script from CNS and with PROCHECK[17] in the CCP4 suite of programs.

Isothermal Titration Calorimetry. Isothermal titration calorimetry (ITC) was used to determine the affinity of QacR for DB75 and DB359. All protein samples were extensively dialyzed into buffer A, and DB75 and DB359 were dissolved into the dialysis buffer directly. Ligand and protein concentrations were determined spectrophotometrically. For the DB75 titration, the concentration of the QacR was 20 μM and the ligand concentration was 961 μM. For the DB359 titration, the concentration of QacR was 10 μM and the concentration of DB359 was 420 μM. Protein and ligand samples were degassed before they were loaded into the cell and syringe of the VP-ITC from MicroCal, Inc. (North Hampton, MA). The stirring speed was set to 300 rpm, and the power was set to 10 μcal/s. Binding experiments were carried out with the protein solution in the cell and the ligand as the injectant and in the reverse mode. Ten microliter injections of were used for data collection. Determination of the binding affinities of DB75 and DB359 for QacR under the conditions used to grow crystals of these complexes was not possible due the inability to solubilize such high concentrations of drug in 2.3 M ammonium sulfate. Data analysis, using a single-site binding model, was performed with the Origin 5.0 package (OriginLab Corporation).

Fluorescence Polarization. Fluorescence polarization (FP) experiments were carried out using a PanVera Beacon polarization system (Invitrogen, Carlsbad, CA). In order to determine the K_d for Et binding to QacR under our crystallization conditions, QacR was titrated into solutions of either 5.0 or 0.5 μM Et in 2.3 M ammonium sulfate and 0.1 M sodium acetate, pH 4.6 (the crystallization condition) or as a control, 0.5 μM Et was added to 50 mM Tris−HCl, pH 7.5, 300 mM NaCl, 50 mM imidazole. The increase in polarization was measured after each addition of QacR into the Et-containing binding buffer and a 30 s incubation period, which ensured equilibrium, was reached. Due to their lack of intrinsic polarization, the affinities of DB75 and DB359 for QacR could not be measured directly using the same experimental approach. Rather, the QacR binding capabilities of DB75 and DB359 under our crystallization conditions were demonstrated using a competition assay, whereby each DB compound was titrated into a solution of a stoichiometric complex of QacR−Et (1 dimer/1 drug) in 2.3 M $(NH_4)_2SO_4$, 0.1 M sodium acetate, pH 4.6. The concentration of each DB stock solution was 125 μM. The decrease in polarization, due to Et dissociation, was measured after addition of an aliquot of either DB75 or DB359. Equilibrium binding was again ensured by a 30 s incubation period. The binding volumes for all FP experiments were 100 μL, and dilution effects were corrected as necessary. All binding assays were carried out at 25 °C. Ethidium was excited at 535 nM, and its polarized emissions were measured at 620 nm. The QacR−Et binding data were plotted using KaleidaGraph (Synergy Software, Reading, PA), and the dissociation constants were determined using the equation $P = \{(P_{bound} - P_{free})[protein]/K_d\} + P_{free}$, where P is the measured polarization, P_{bound} is the maximum polarization of QacR-bound Et, P_{free} is the polarization of Et before QacR is added, [protein] is the protein concentration at a given polarization measurement, and K_d is the equilibrium dissociation constant.

The concentration of each drug was calculated using the experimentally determined absorbance maximum (A_{360} for DB75 and A_{327} for DB359) and extinction coefficients of 36 600 $M^{-1}\cdot cm^{-1}$ (for DB75) and 28 570 $M^{-1}\cdot cm^{-1}$ (for DB359).

Results and Discussion

The binding affinity of each DB compound for the QacR dimer was determined by ITC, which gave equilibrium dissociation constants of 18 ± 3 μM and 15 ± 2 μM for DB75 and DB359, respectively (Figure 2). Such affinities are lower than those of many QacR inducers, which range from 0.15 to 187 μM,[5,6,18] but are similar to the diamidines, phenamidine and amicarbalide, which display dissociation constants of 9 and 16 μM, respectively.[18] As expected, the thermodynamic parameters of binding of each DB compound to QacR are similar, with DB75 displaying an enthalpic contribution of ΔH(DB75) = −19 ± 2 kcal/mol and DB359 a ΔH(DB359) = −21 ± 4 kcal/mol. Each displayed a similar entropic contribution as well with ΔS(DB75) = −43 cal·mol·deg^{-1} and ΔS(DB359) = −49 cal·mol·deg^{-1}. These losses in entropy offset the larger enthalpic gains upon binding of the DBs to QacR and hence result in the observed relatively modest affinities. The stoichiometries of drug binding were slightly elevated, ranging from 1.2 to 1.4 (drug/QacR dimer), most likely due to small errors in the estimation of drug and protein concentrations or specific activities.

(17) Laskowski, R. A.; MacArthur, M. W.; Moss, D. S.; Thornton, J. M. *J. Appl. Crystallogr.* **1993**, *26*, 283.

(18) Grkovic, S.; Hardie, K. M.; Brown, M. H.; Skurray, R. A. *Biochemistry* **2003**, *42*, 15226−15236.

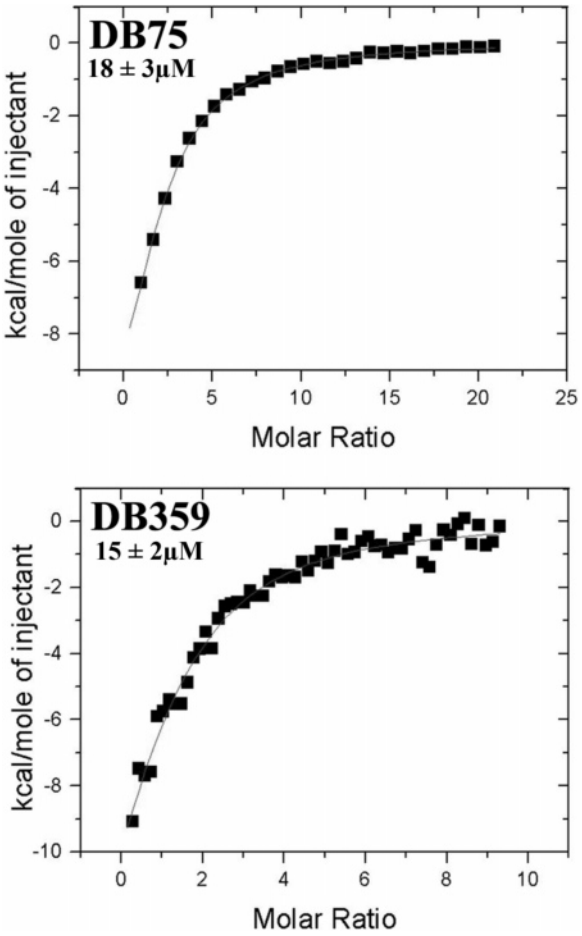

Figure 2. Integrated binding isotherms of QacR−DB75 and QacrR−DB359.

In order to place these binding data in a structural context, the crystal structures of the QacR−DB75 and the QacR−DB359 complexes were determined to 2.80 Å resolution (Table 1).[19] As expected, the drug-bound subunit of QacR takes the canonical drug-bound conformation (Figures 3 and 4). Despite taking the drug-bound conformation, neither the QacR−DB75 complex structure nor the QacR−DB359 complex structure displays any continuous electron density in the binding pocket that would describe unambiguously either a single or highly preferred binding site for each drug (Figure 5). Although the QacR−DB359 complex had some continuous patches of electron density in the binding pocket, fitting the drug or parts of the drug into these densities did not result in a significant improvement to the refinement statistics. On the other hand, these parameters did not worsen, and thus, these patches of electron density indicate the likely general locations of DB359 binding. Similar fitting experiments in the QacR−DB75 complex electron density had a more deleterious effect on the refinement statistics. In both cases, lowering the resolution of the data to 3.0 Å did not improve or clarify the electron density in the multidrug-binding pocket. Thus, each ligand does not appear to bind QacR in a single preferred site.

To glean some understanding of the DB359−QacR interaction, three sterically allowable, with respect to protein−drug steric clash, but mutually exclusive drug complexes were fit manually into $2F_o - F_c$ composite omit electron density (Figure 5A). In all three binding modes DB359 spans the length of the multidrug-binding pocket and can utilize binding determinants of the Et binding pocket (residues Y103 and E120), the R6G pocket (residues W61 and Y93), and the gatekeeper residue Y123.[6] Each binding mode resembles that of hexamidine, a longer aromatic diamidine.[7] There is no experimental evidence, particularly the relocation of certain side chains, that indicates DB359 and pentamidine bind QacR similarly, a finding which reflects the rigidity of DB359 and, thus, its inability to follow the winding binding site of the similarly sized pentamidine.[7]

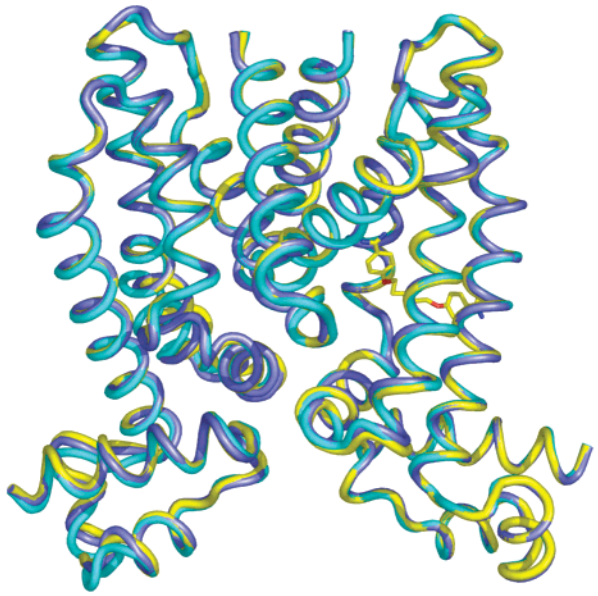

Figure 3. Overlay of the QacR−pentamidine (yellow), QacR−DB75 (cyan), and QacR−DB359 (dark blue) complexes. The structures are identical with root mean squared deviations of less than 0.4 Å. Pentamidine is shown as a stick model, whereby carbon, nitrogen, and oxygen atoms are colored yellow, blue, and red, respectively.

Similarly DB75 was placed into the discontinuous electron densities in the drug-binding pocket in several overlapping but sterically allowable orientations (Figure 5B). Like DB359, DB75 can span the binding pocket and interact with residues of the R6G and Et pockets, although at least one modeled binding mode (in blue) that differs significantly from the rest can be readily placed without steric clash. Regardless, we are able to limit the binding loci of DB75 using as guides the positions of QacR side chains that have been shown to interact with other drugs in our previous studies.[5−7] These residues orient themselves in a drug-dependent manner to accommodate drug shape and maximize interactions. One such residue is Y123, which has been shown to be involved in stacking interactions with all QacR-bound drugs. In order to stack with drugs, the phenol side chain takes different orientations that are dependent upon whether the R6G or Et binding site is occupied.[5−7] Unlike the QacR−DB359 complex, the side chain of this residue of the QacR−DB75 complex is disordered completely with no visible $2F_o - F_c$ composite omit electron density even when contoured as low as 0.5σ (Figure 5). The disorder of this aromatic side chain indicates multiple orientations are taken and strongly implies that these multiple conformations are taken in order to interact with drug binding in multiple positions. Other key residues are also found in multiple, although sometimes more

(19) The coordinates and structure factors for the QacR−DB359 and QacR−DB75 complexes have been deposited in the Protein Data Bank (PDB) with the PDB accession numbers 2HQ5 and 2DTZ, respectively.

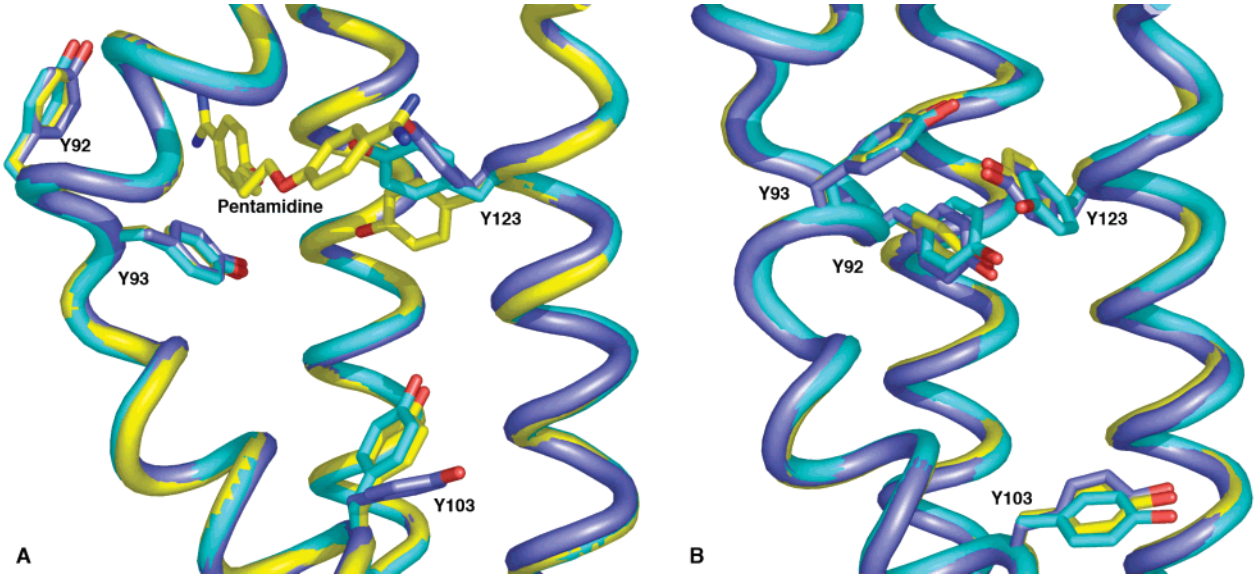

Figure 4. View of the QacR multidrug-binding pocket in its drug-bound and drug-free conformations. (A) Overlay of the QacR−pentamidine (yellow), QacR−DB75 (cyan), and QacR−DB359 (dark blue) complexes in the "opened" or drug-bound conformation. Key drug interacting side chains, including Y92, Y93, Y103, and Y123 are displayed as stick models as is pentamidine. Note the identical locations of the Y92 and Y93 side chains, which have been expelled from the interior of the protein by drug binding. (B) Overlay of the drug-free QacR dimers (the "closed" conformation) that are shown in panel A and found in the asymmetric unit of all drug-bound QacR dimers (refs 5−7). Note well the nearly identical, internal positions of residues Y92 and Y93 and the lack of the coil-to-helix transition, two critically distinctive features of drug-free QacR.

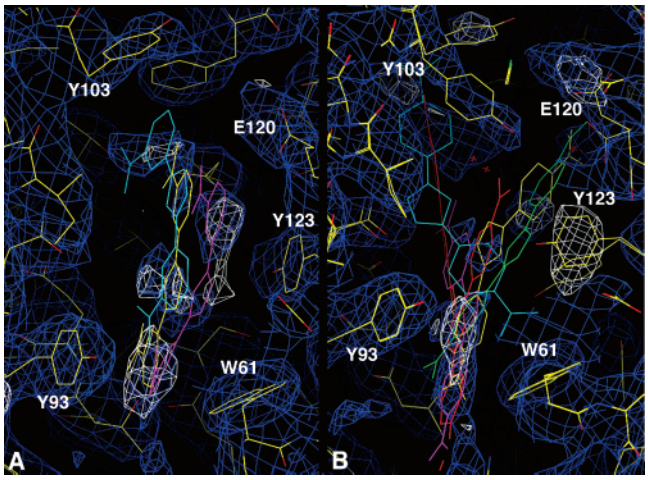

Figure 5. Plausible binding modes of DB359 and DB75 to QacR. (A) Modeled QacR−DB359 complexes. (B) Modeled QacR−DB75 complexes. Each modeled drug is depicted as a stick in rainbow coloring. The $2F_o - F_c$ composite omit electron density maps, contoured at 1σ (blue mesh), and the $F_o - F_c$ difference electron density maps, contoured at 3σ (white mesh), are shown. No attempts to optimize drug binding have been made, in part because several side chains of the multidrug-binding pockets are missing. Note the alternate positions of Y103, Y123, and E120 in the QacR−DB75 complex.

discrete, conformations and include residues Y103 and E120, which have electron densities indicative of at least two conformations (Figure 5B). Multiple side-chain orientations, which facilitate protein−drug interaction, are also observed in the human xenobiotic-binding transcription activator, the Pregnane X Receptor (PXR) and are likely a binding characteristic of all multidrug-binding proteins.[20,21]

We are able to discount the idea that there is little or no DB75 or DB359 in the drug-binding pocket, i.e., there is discrete drug binding but its occupancy is too low or zero due to diffusion of drug from the binding pocket during or post crystallization, thus leaving no discernible electron density. First and highly compelling, only the drug-bound subunit of QacR can undergo the drug-induced and drug-stabilized coil-to-helix transition, which is the distinctive feature of the induced conformation of this transcription repressor. Indeed, the subunits of a drug-free QacR dimer that fortuitously crystallizes in the same asymmetric unit as the drug-bound QacR dimer are in the "closed" conformation, in which there is no coil-to-helix transition, no tyrosine expulsion, and thus no formation and exposure of the aromatic multidrug-binding pocket. Furthermore, the drug-binding pocket of the drug-free subunit of the drug-bound QacR dimer (n.b., the stoichiometry of drug binding is one drug per QacR dimer) is also completely closed. That is to say, drug-free QacR does not take or rather cannot maintain its open drug-bound conformation in the absence of drug. Clearly, an open but empty multidrug-binding pocket would be energetically unfavorable as tens of aromatic and aliphatic residues, which constitute part of hydrophobic core of QacR, would be exposed to the highly polar and charged environment of the crystallization solution, which contains 2.3 M ammonium sulfate. Third, the concentrations of DB75 and DB359 in the crystallization drops are high relative to their experimentally determined binding constants (at least 10−30-fold above K_d or added to protein solutions in saturating quantities (see the Materials and Methods)). Moreover, the addition of solid drug to crystallization drops at the start of the crystallization experiment does not change the nature of the experimental electron density (data not shown). Finally, if indeed each drug did diffuse from the binding pocket and somehow this hydrophobic binding pocket did not close, it would be very difficult to reconcile the observation that the side chains of several residues in the multidrug-binding pocket, including E90, Y103, and Y123, take different conformations

(20) Watkins, R. E.; Wisely, G. B.; Moore, L. B.; Collins, J. L.; Lambert, M. H.; Williams, S. P.; Willson, T. M.; Kliewer, S. A.; Redinbo, M. R. *Science* **2001**, *292*, 2329−2333.
(21) Watkins, R. E.; Maglich, J. M.; Moore, L. B.; Wisely, G. B.; Noble, S. M.; Davis-Searles, P. R.; Lambert, M. H.; Kliewer, S. A.; Redinbo, M. R. *Biochemistry* **2003**, *42*, 1430−1438.

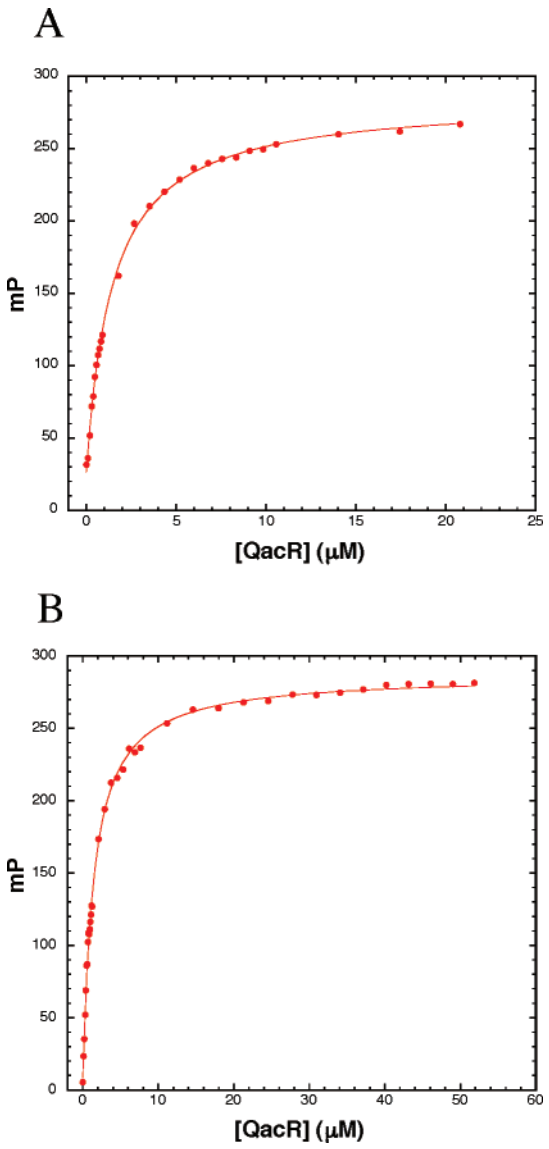

Figure 6. Binding isotherms of QacR and Et in crystallization and neutral buffer conditions. (A) QacR binding to Et in 2.3 M ammonium sulfate, 0.1 M sodium acetate, pH 4.6. The Et concentration was 5.0 μM, but no significant difference in K_d (1.40−2.0 μM) is observed when the Et concentration is lowered to 0.5 μM. (B) QacR binding to Et in 50 mM Tris, pH 7.5, 300 mM NaCl, and 50 mM imidazole. The Et concentration is 0.5 μM. The change in Et polarization, given in units of millipolarization (mP), was recorded after each titration of QacR into the Et-containing solutions and plotted as solid red circles.

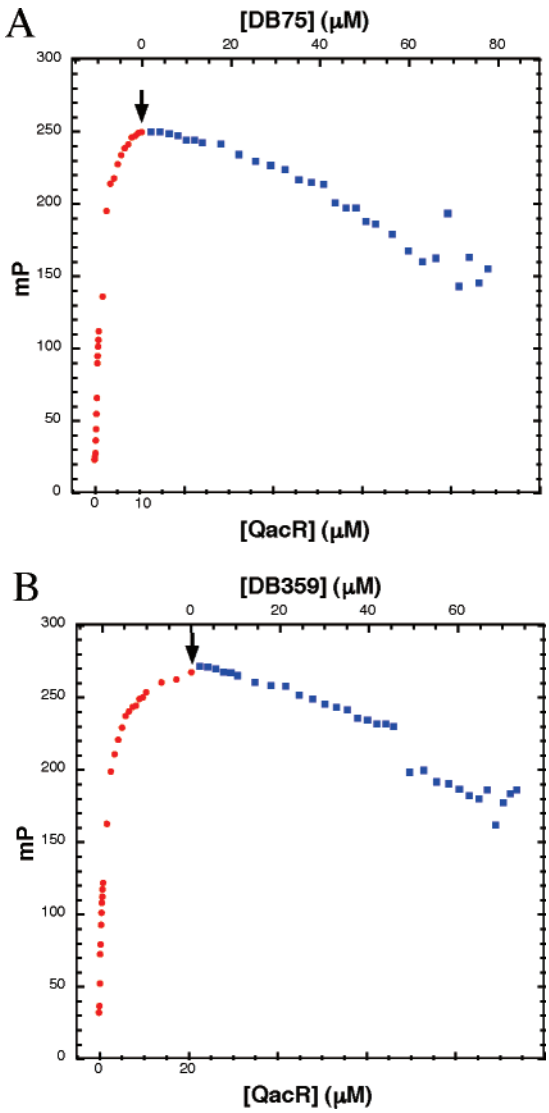

Figure 7. QacR binding competition experiments between Et and DB75 and DB359. (A) QacR binding to Et (solid red circles) followed by the addition (after 10 μM QacR had been added and demarked by the black vertical arrow) of DB75 (solid blue squares). (B) QacR binding to Et (solid red circles) followed by the addition (after 20 mM QacR had been added and demarked by the black vertical arrow) of DB359 (solid blue squares). Both binding isotherms were carried out in 2.3 M ammonium sulfate, 0.1 M sodium acetate, pH 4.6. The Et concentration was 5 μM for the initial binding to QacR in both experiments. All titrations of DB75 and DB359 were made from initial stock concentrations of 125 μM. The change in Et polarization, given in units of millipolarization (mP), was recorded after each titration of QacR into the Et-containing solutions and then after addition of each aliquot of DB75 or DB359.

depending upon which drug is in the crystallization condition. Without drug in the binding pocket, one should expect the same conformational flexibility and hence no differences.

We are unable to measure the binding affinity of DB75 or DB359 for QacR by ITC under our crystallization condition (2.3 M ammonium sulfate, 0.1 M sodium acetate, pH 4.6) due to insurmountable aggregation problems. Intrinsic fluorescence quenching of QacR or the compounds could not be utilized due to severe inner filter effects. However, binding studies using an FP-based assay were possible and provided additional evidence that all tested QacR ligands, including DB75 and DB359, bind this repressor protein with high affinity in 2.3 M ammonium sulfate, 0.1 M sodium acetate, pH 4.6. As a control, the binding affinity of QacR for Et was determined first under neutral conditions (50 mM Tris−HCl, pH 7.5, 300 mM NaCl, 50 mM imidazole) and then under our crystallization conditions (2.3 M ammonium sulfate, 0.1 M sodium acetate, pH 4.6). Under each condition, excellent binding isotherms were generated (Figure 6). The equilibrium binding constant in the "neutral" buffer is 1.47 μM and in the crystallization buffer, 1.40 μM. Thus, the crystallization buffer has a no deleterious effect on K_d. Similar results, i.e., no significant changes, were found when the equilibrium binding constants for R6G was determined under these two experimental conditions (data not shown), and by inference we would expect the same finding for DB75 and DB359.

Unfortunately, we were unable to do FP-based binding assays to determine the binding affinities of QacR for DB75 and DB359

in our crystallization buffer directly, as neither of these compounds displays any measurable FP. In lieu, we carried out "knock off/competition" experiments, whereby either DB75 or DB359 was titrated into a solution of stoichiometrically bound QacR−Et complex in our crystallization conditions. The data reveal that each DB compound was able to bind QacR as demonstrated by the release of Et and resulting decreased Et polarization (Figure 7). The data are also consistent with the ∼10-fold tighter binding of Et to QacR than either DB compound, which results in the more gradual decrease in Et polarization as a function of increasing DB concentration. The titrations could not be completed, as defined by bringing the polarization of the Et back to its initial value when no QacR is present, due to precipitation of one or more of the binding components at higher DB concentrations. Regardless, these data show DB75 and DB359 can bind to QacR in the crystallization buffer and support the contention that the lack of discrete electron density for DB75 and DB359 in the crystal structures described here is not a simple matter of exceedingly low occupancy of one favored binding site or diffusion of drug away from the multidrug-binding pocket, which then somehow remains open despite exposing multiple hydrophobic residues. Moreover, the saturating concentration of DB75 is ∼80 μM and of DB359 over 400 μM using the crystallization conditions, which, assuming similar QacR−DB equilibrium dissociation constants in this and the neutral buffer A conditions (as demonstrated for Et and R6G), indicates the amount of soluble DB75 and DB359 in the crystallization drop is greater than 10−40 times their K_d's on a one drug per dimer basis. Thus, we conclude that there are sufficient concentrations of DB75 and DB359 available in the crystallization buffer solution to bind QacR in high occupancy such that any single or highly preferred binding site would be readily observed. Furthermore, we conclude that DB75 and DB359 utilize multiple, overlapping and apparently isoenergetic modes of binding to QacR.

The precise number of binding modes taken by DB359 and DB75 is unknown. PXR binds the cholesterol-lowering drug SR12813 in three separate but overlapping orientations in its multidrug-binding pocket, which is similar in volume to that of QacR.[5,20] As expected, the electron density of each SR12813 is significantly weakened in nonoverlapping areas. By analogy, multiple, isogenic bindings of DB75 or DB359 to QacR would result in a loss of discrete electron density, and thus it is tempting to speculate that given their poor experimentally observed residual electron densities, DB75 and DB359 use at least three different binding modes. Somewhat surprising, QacR shows no correlation between drug-binding affinity and the experimentally observed electron density of the drug. For example, the experimentally determined binding affinity of proflavin for QacR is ∼42 μM, which is 4−5-fold lower than DB75 and DB359.[6] Yet proflavin takes a single binding mode and is completely resolved in the initial 2.89 Å resolution electron density difference map, despite a concentration of only 100 μM drug having been added to the crystallization drop.[6] Inversely PXR has high affinity for SR12813 (K_d = 41 nM), but the drug is bound in three orientations with poorly defined electron densities.[20] Thus, for at least QacR and perhaps other multidrug-binding proteins, ligand affinity does not always correlate with discrete electron density.

In conclusion, the rigid aromatic diamidines DB75 and DB359 utilize an unknown number of overlapping apparently isoenergetic modes of binding. In turn, such binding indicates that the multidrug-binding pocket of QacR, which is rich in aromatic and drug-charge neutralizing acidic residues, is chemically redundant. Such redundancy appears to be exploited by some drugs to bind to their target proteins in more than one thermodynamically equivalent orientation.

Acknowledgment. This work was supported by NIH Grant AI48593. We thank Dr. Corie Ralston for facilitating data collection at ALS Beamline 8.2.1 (Berkeley, CA). DB75 and DB359 were kindly provided by Drs. David W. Boykin and W. David Wilson of Georgia State University.

JA072576V